Supporting Information

Multi-Mode Emission Color Tuning of Dithieno[3,2-*b*:2',3'-*d*]arsoles

Hiroaki Imoto, Ikuo Kawashima, Chieko Yamazawa, Susumu Tanaka and Kensuke Naka*

Faculty of Molecular Chemistry and Engineering, Graduate School of Science and Technology, Kyoto Institute of Technology, Goshokaido-cho, Matsugasaki, Sakyo-ku, Kyoto 606-8585, Japan.

Contents:
1. NMR spectra
2. Crystallographic data
3. Optical data
4. Electronic properties

1. NMR spectra
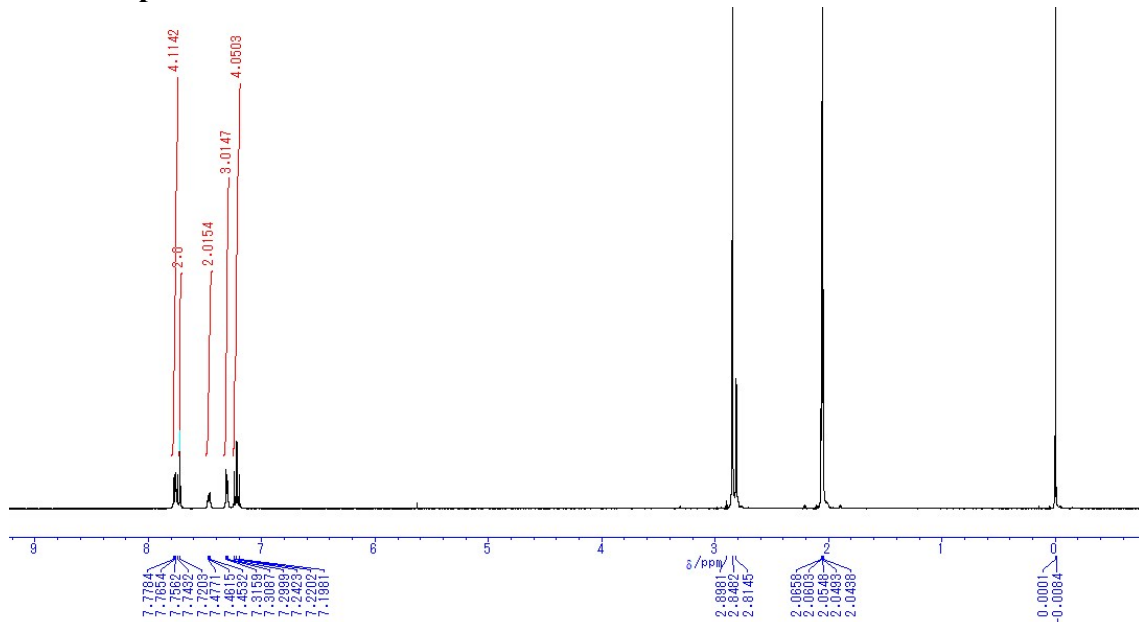
**Figure S1.** ^{1}H-NMR spectra (400 MHz) of **4b** in acetone-d_6.
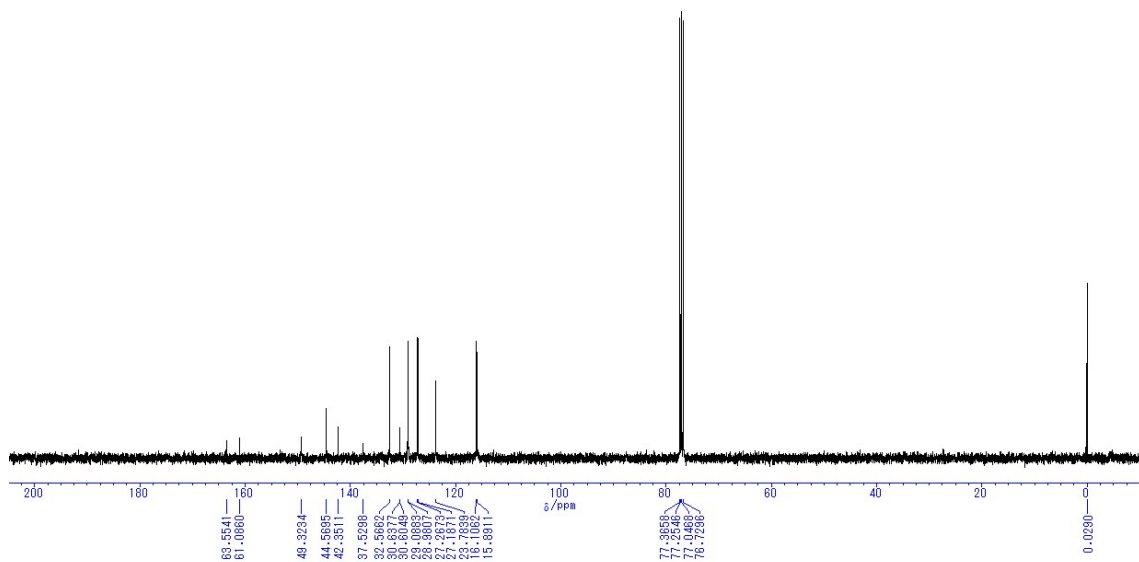
Figure S2. ^{13}C-NMR spectra (100 MHz) of **4b** in CDCl$_3$.
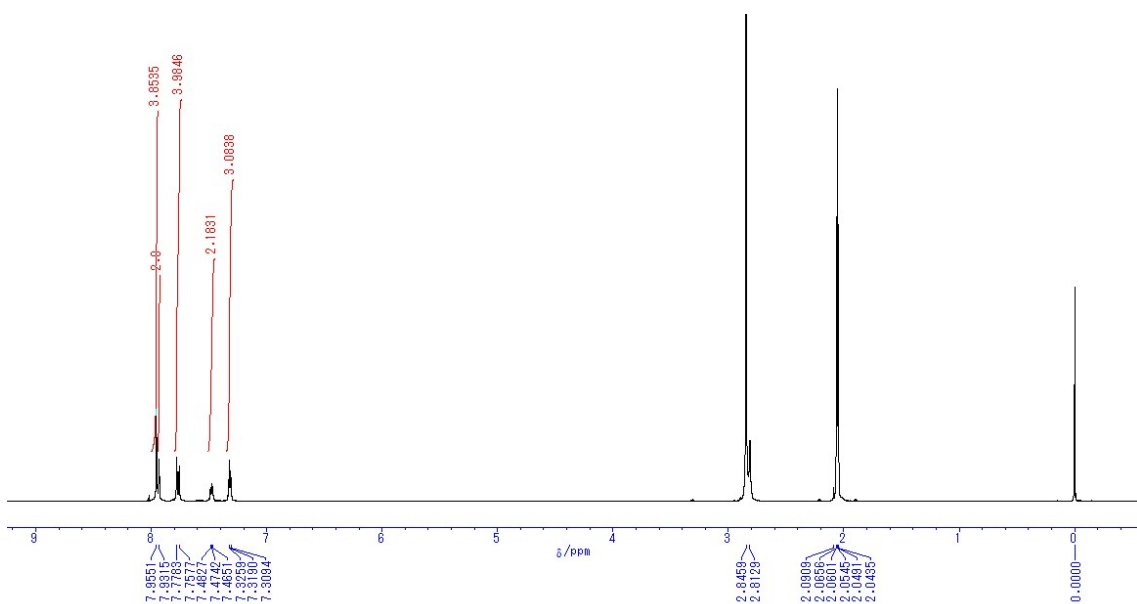
Figure S3. ^{1}H-NMR spectra (400 MHz) of **4c** in acetone-d_6.
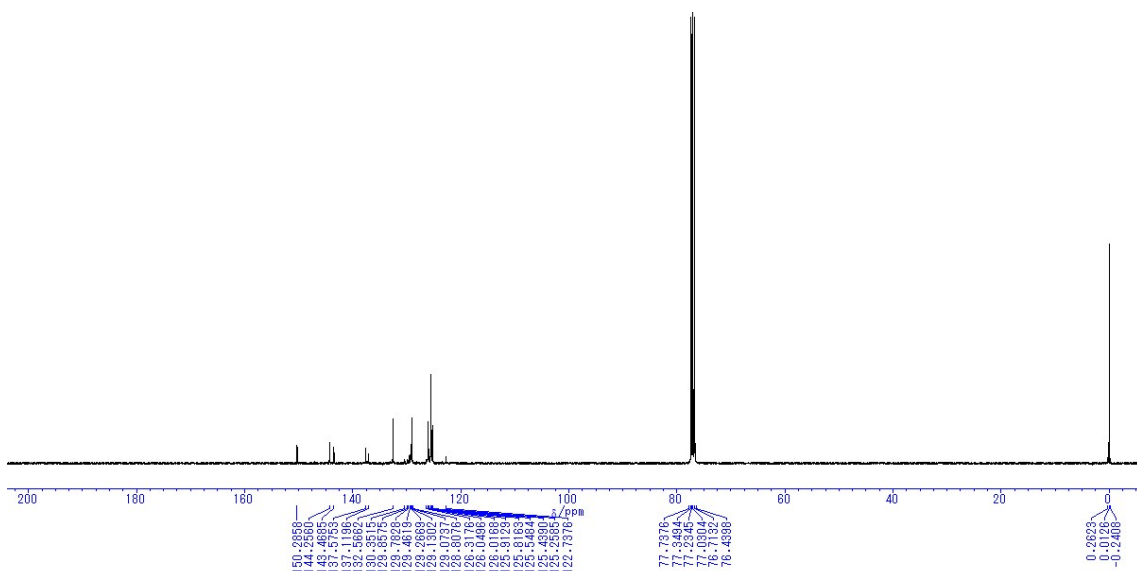
Figure S4. ^{13}C-NMR spectra (100 MHz) of **4c** in CDCl$_3$.
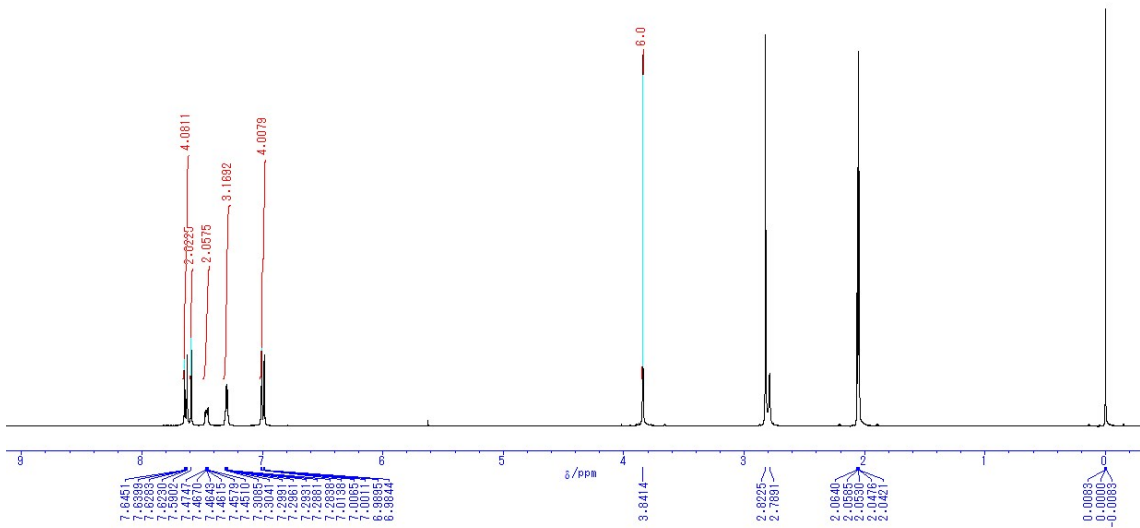
Figure S5. ^{1}H-NMR spectra (400 MHz) of **4d** in acetone-d_6.
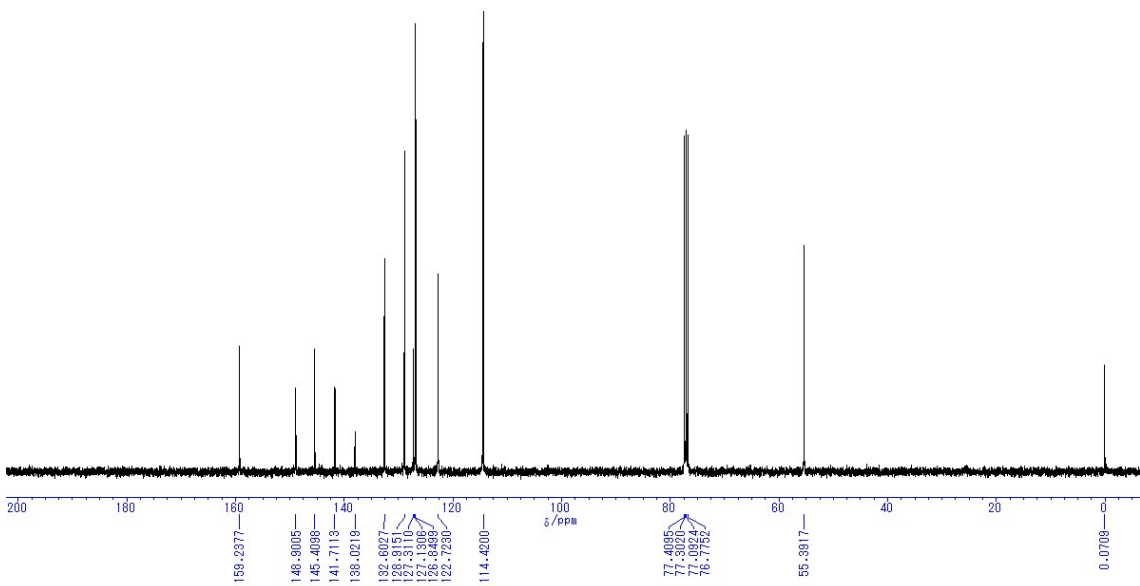
Figure S6. ^{13}C-NMR spectra (100 MHz) of **4d** in CDCl$_3$.
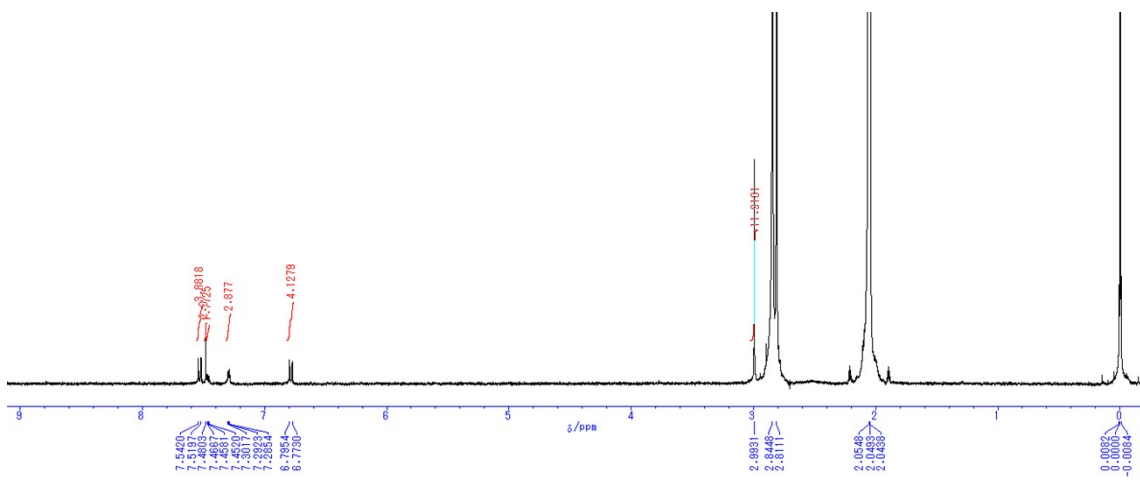
Figure S7. ^{1}H-NMR spectra (400 MHz) of **4e** in acetone-d_6.
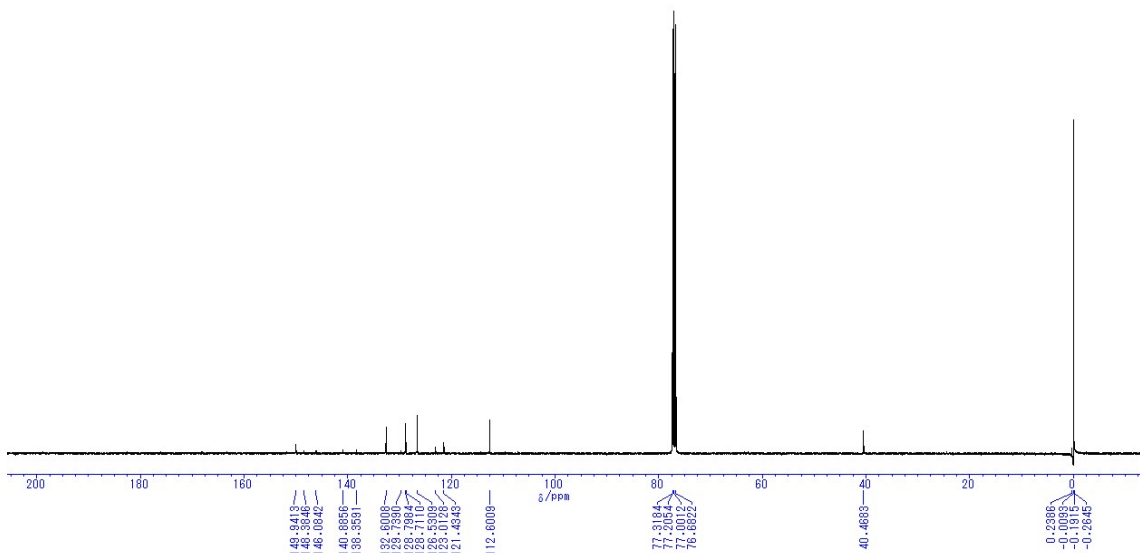
Figure S8. ^{13}C-NMR spectra (100 MHz) of **4e** in CDCl$_3$.
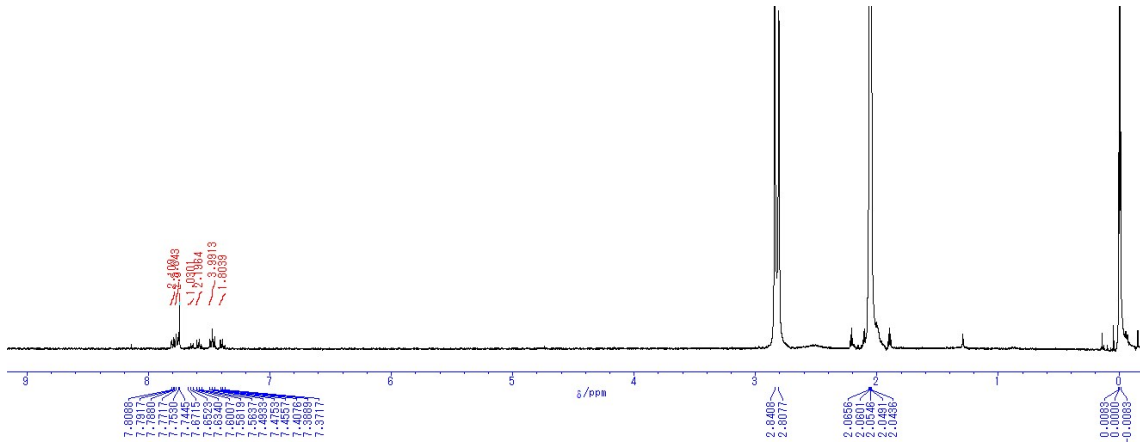
**Figure S9.** ^{1}H-NMR spectra (400 MHz) of **5** in acetone-d_6.
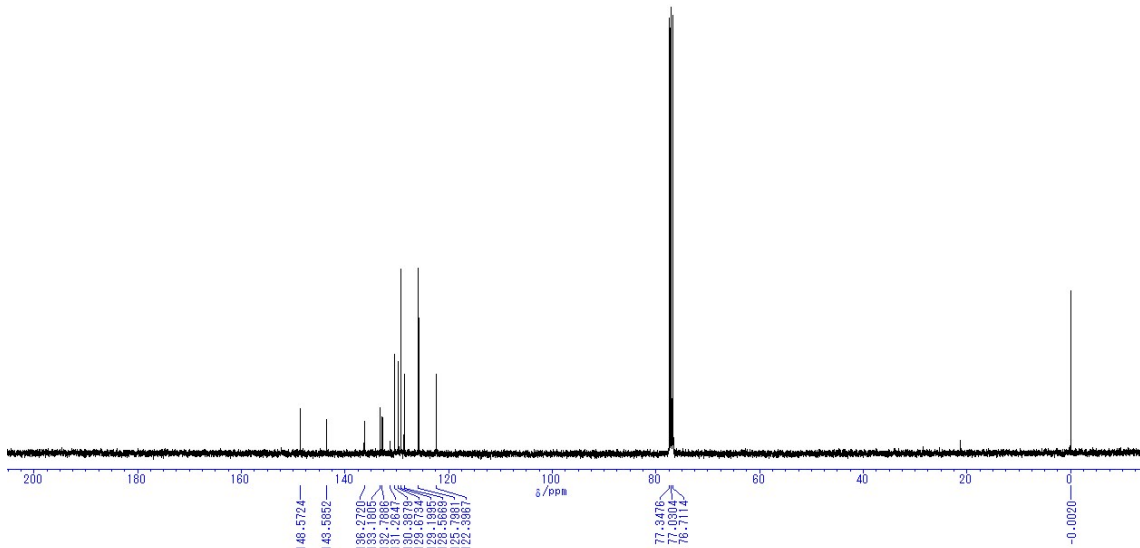
Figure S10. ^{13}C-NMR spectra (100 MHz) of **5** in CDCl$_3$.
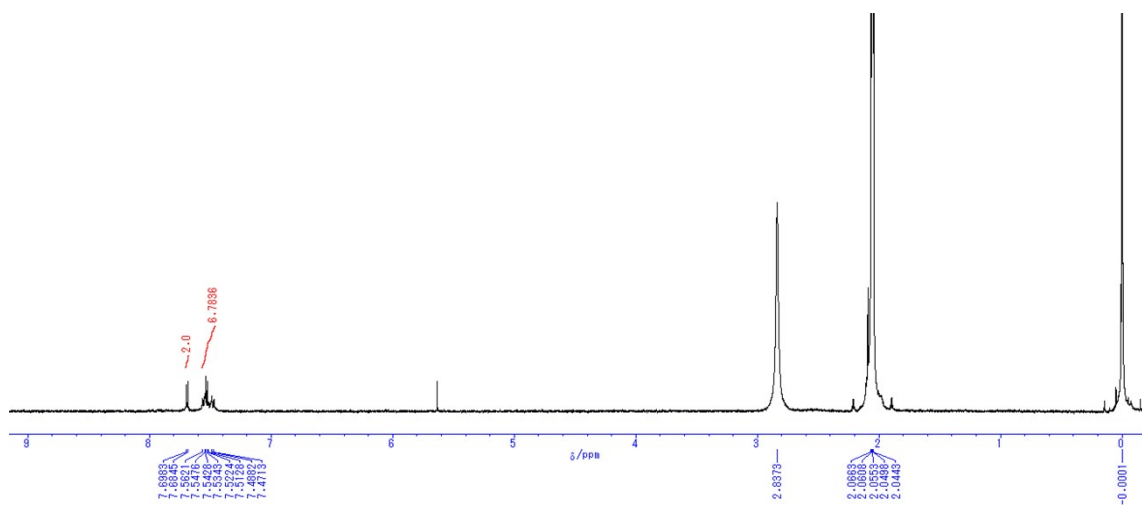
Figure S11. ^{1}H-NMR spectra (400 MHz) of **6** in acetone-d_6.
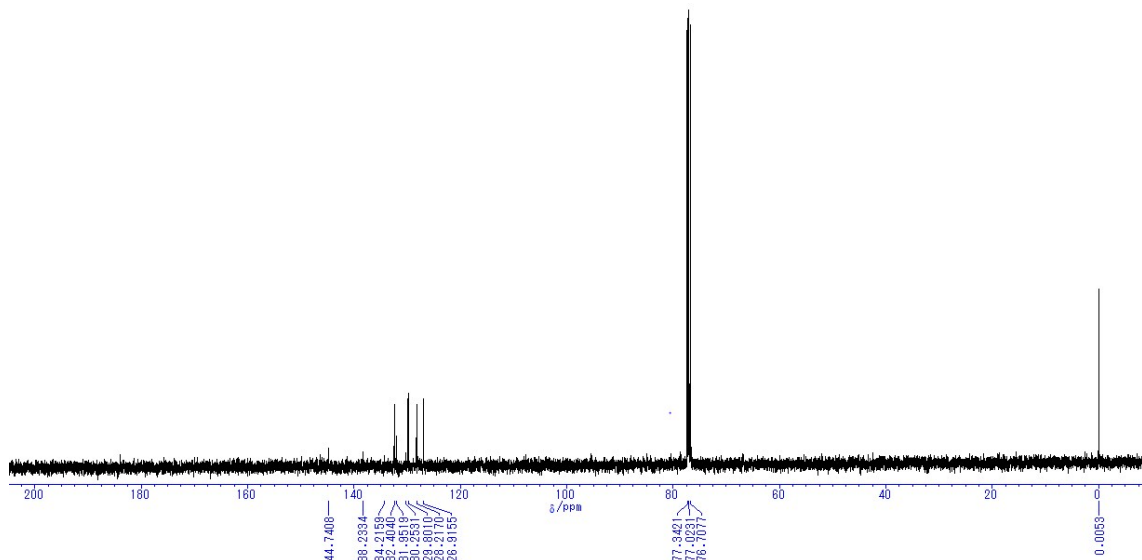
Figure S12. ^{13}C-NMR spectra (100 MHz) of **6** in CDCl$_3$.
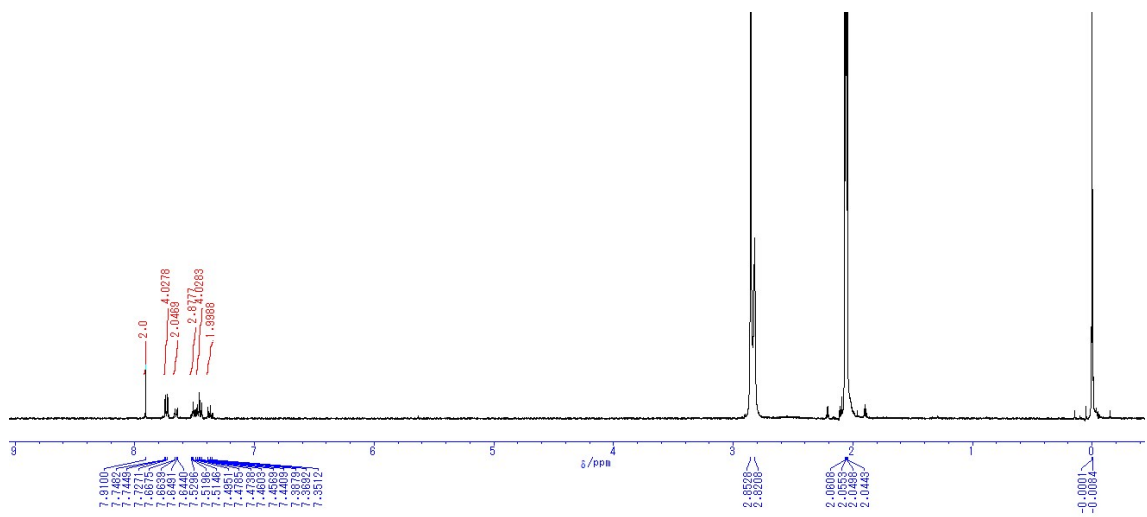
**Figure S13.** ^{1}H-NMR spectra (400 MHz) of **7** in acetone-d_6.
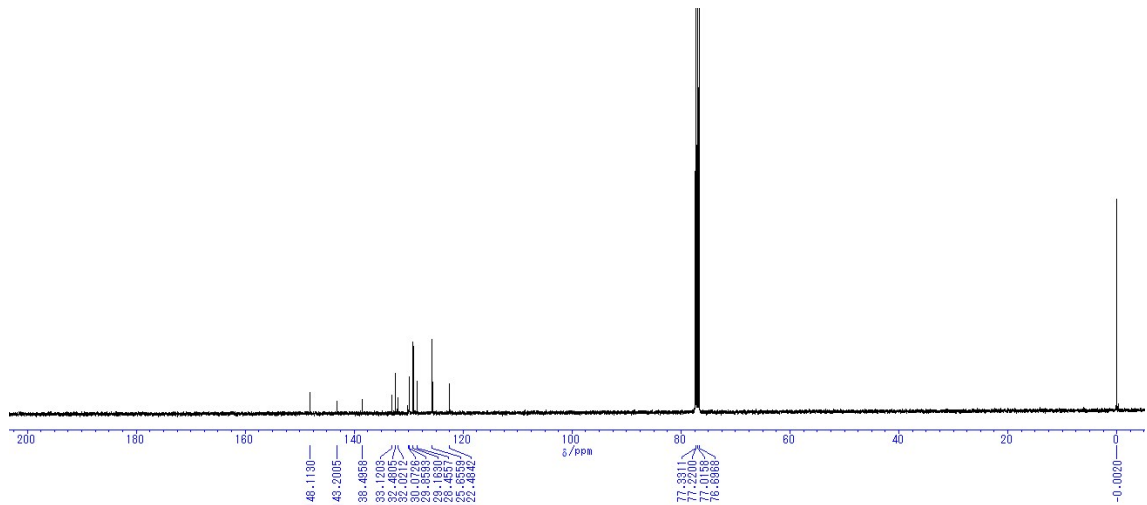
Figure S14. ^{13}C-NMR spectra (100 MHz) of **7** in CDCl$_3$.

2. Crystallographic data

Table S1. Crystallographic Data of **4b** and **4d**.

	4b	4d
Crystal data		
Empirical Formula	$C_{26}H_{15}AsF_2S_2$	$C_{28}H_{21}AsO_2S_2$
Formula Weight	504.44	528.51
Crystal Dimension, mm^3	$0.303 \times 0.122 \times 0.033$	$0.220 \times 0.080 \times 0.020$
Crystal System	triclinic	triclinic
Space Group	P-1	P-1
a, Å	14.08240(2)	5.340(8)
b, Å	14.34260(18)	11.414(18)
c, Å	17.9855(5)	19.25(3)
α, deg	74.420(19)	88.62(3)
β, deg	73.737(16)	87.63(4)
γ, deg	74.178(19)	84.27(3)
Volume, Å^3	3281.7(4)	1166(3)
D_{calcd}, g cm^{-3}	1.531	1.505
Z	6	2
F(000)	1524.00	540.00
Data Collection		
Temperature, deg	23.0	23.0
2θmax, deg	55.0	55.2
Tmin/Tmax	0.801 / 0.943	0.785 / 0.967
Refinement		
No. of Observed Data	14963	5198
No. of Parameters	838	298
R1^a, wR2^b	0.0601, 0.1657	0.0703, 0.1976
Goodness of Fit Indictor	1.041	1.045

^{a}R1 = Σ | |Fo| - |Fc| | / Σ |Fo| ^{b}wR2 = [Σ w ((Fo^2-Fc^2)^2 / Σ w (Fo^2)^2]$^{1/2}$ w = [σ^2(Fo^2)]$^{-1}$

CCDC # 1546576 (**4b**), 1546573 (**4d**)

Table S2. Crystallographic Data of **4e** and **5**.

	4e	5
Crystal data		
Empirical Formula	$C_{30}H_{27}AsN_2S_2$	$C_{26}H_{17}AsOS_2$
Formula Weight	554.60	484.46
Crystal Dimension, mm^3	$0.221 \times 0.136 \times 0.032$	$0.310 \times 0.120 \times 0.100$
Crystal System	monoclinic	triclinic
Space Group	$P2_1/c$	P-1
a, Å	10.1843(15)	9.113(7)
b, Å	26.678(4)	11.080(9)
c, Å	10.0150(16)	13.736(10)
α, deg	-	102.917(7)
β, deg	99.375(7)	91.848(10)
γ, deg	-	112.471(6)
Volume, $Å^3$	2684.7(7)	1238.5(17)
D_{calcd}, g cm^{-3}	1.372	1.299
Z	4	2
F(000)	1144.00	492.00
Data Collection		
Temperature, deg	23.0	23.0
2θmax, deg	55.0	55.1
Tmin/Tmax	-	0.695/0.856
Refinement		
No. of Observed Data	6153	5548
No. of Parameters	316	271
R1[a], wR2[b]	0.0812, 0.1595	0.0446 / 0.1387
Goodness of Fit Indictor	1.023	0.844

[a]R1 = $\Sigma \,| \,|Fo| - |Fc| \,| \,/ \,\Sigma \,|Fo|$ [b]wR2 = $[\,\Sigma \,w \,((Fo^2-Fc^2)^2 / \Sigma \,w \,(Fo^2)^2 \,]^{1/2}$ w = $[\sigma^2(Fo^2)]^{-1}$

CCDC # 1546575 (**4e**), 1546574 (**5**)

**Table S3.** ORTEP drawing (ellipsoids at 50% probability), selected distances, and angles of **4b**.
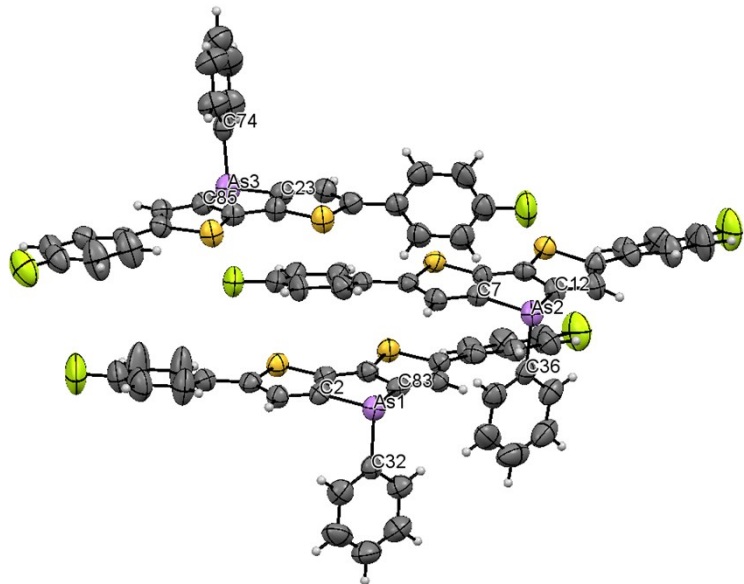
distances (Å)		angles (°)	
As(1)-C(32)	1.962(5)	C(83)-As(1)-C(2)	85.9(2)
As(1)-C(2)	1.957(6)	C(2)-As(1)-C(32)	95.5(2)
As(1)-C(83)	1.947(5)	C(32)-As(1)-C(83)	98.6(2)
As(2)-C(36)	1.968(5)	C(7)-As(2)-C(12)	85.2(2)
As(2)-C(7)	1.955(6)	C(7)-As(2)-C(36)	95.3(2)
As(2)-C(12)	1.946(5)	C(36)-As(2)-C(12)	99.9(2)
As(3)-C(74)	1.945(5)	C(85)-As(3)-C(23)	85.4(2)
As(3)-C(85)	1.948(5)	C(23)-As(3)-C(74)	98.7(2)
As(3)-C(23)	1.949(6)	C(74)-As(3)-C(85)	101.3(2)

**Table S4.** ORTEP drawing (ellipsoids at 50% probability), selected distances, and angles of **4d**.
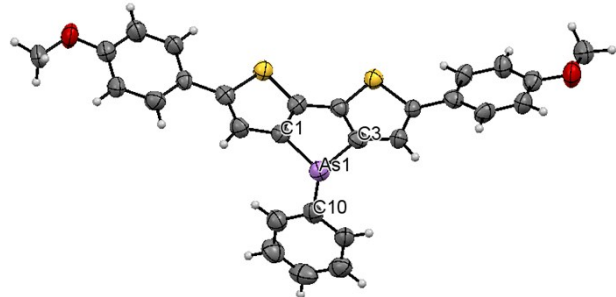
distances (Å)		angles (°)	
As(1)-C(10)	1.968(8)	C(1)-As(1)-C(3)	85.3(3)
As(1)-C(1)	1.937(7)	C(3)-As(1)-C(10)	97.1(3)
As(1)-C(3)	1.947(7)	C(1)-As(1)-C(10)	98.7(3)

Table S5. ORTEP drawing (ellipsoids at 50% probability), selected distances, and angles of **4e**.
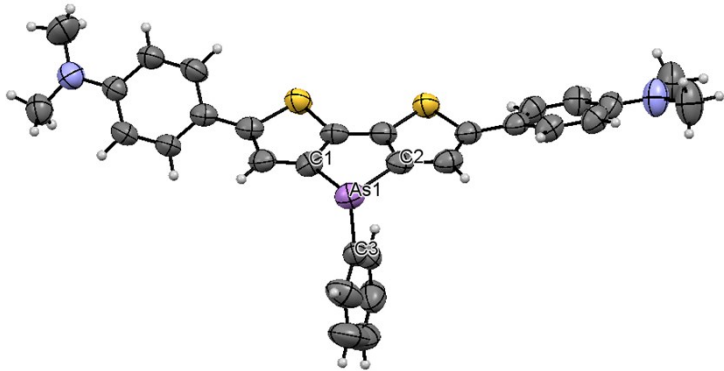
distances (Å)		angles (°)	
As(1)-C(3)	1.974(6)	C(1)-As(1)-C(2)	85.8(2)
As(1)-C(1)	1.958(6)	C(1)-As(1)-C(3)	98.1(2)
As(1)-C(2)	1.962(5)	C(2)-As(1)-C(3)	98.7(2)

Table S6. ORTEP drawing (ellipsoids at 50% probability), selected distances, and angles of **5**.
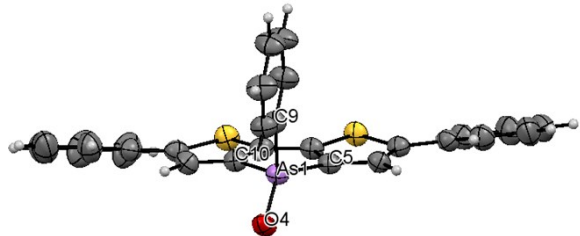
| distances (Å)		angles (°)	
As(1)-O(4)	1.650(3)	O(4)-As(1)-C(9)	115.5(1)
As(1)-C(9)	1.906(4)	O(4)-As(1)-C(5)	124.6(1)
As(1)-C(5)	1.936(3)	O(4)-As(1)-C(10)	110.1(1)
As(1)-C(10)	1.941(4)	C(5)-As(1)-C(10)	88.4(1)
		C(5)-As(1)-C(9)	106.9(1)
		C(10)-As(1)-C(9)	107.1(1)
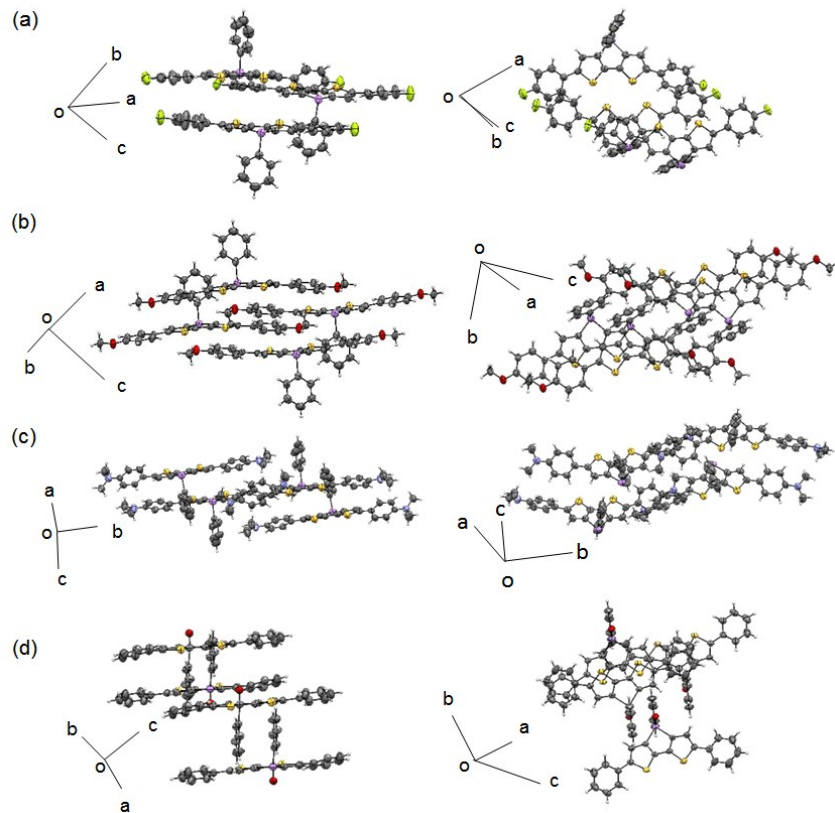
Figure S15. Packing structures of (a) **4b**, (b) **4d**, (c) **4e**, and (d) **5**.

3. Optical data
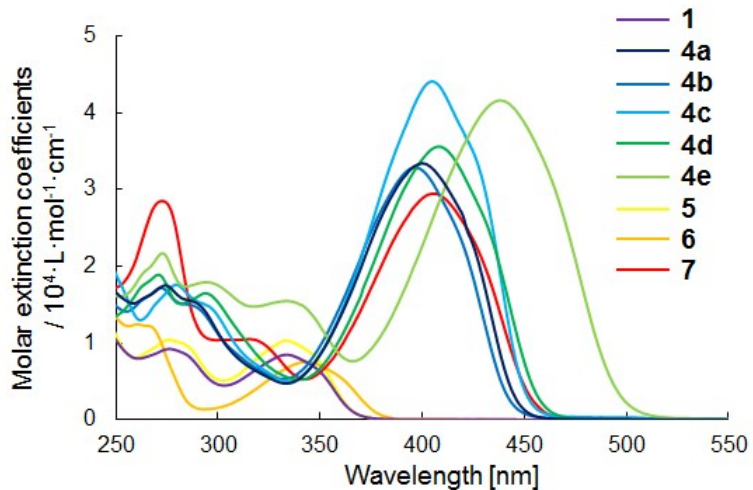
**Figure S16.** UV-vis absorption spectra of **1**, **4a-e**, and **5-7** (1.0×10^{-5} M in CH_2Cl_2).
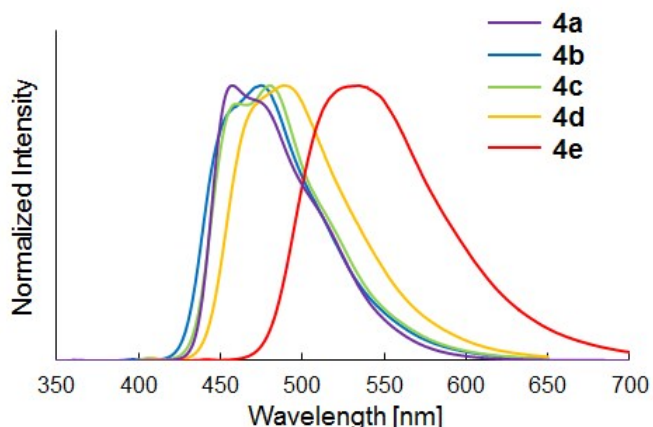
Figure S17. PL spectra of **4a-e** (1.0×10^{-5} M in CH_2Cl_2).
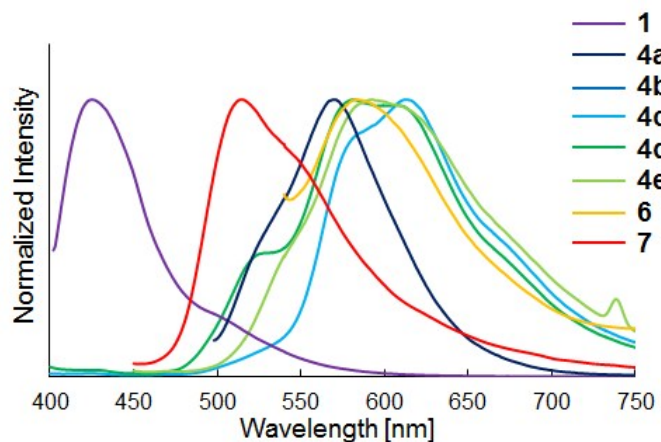
**Figure S18.** PL spectra of **1**, **4a-e**, **6**, and **7** in the solid states.
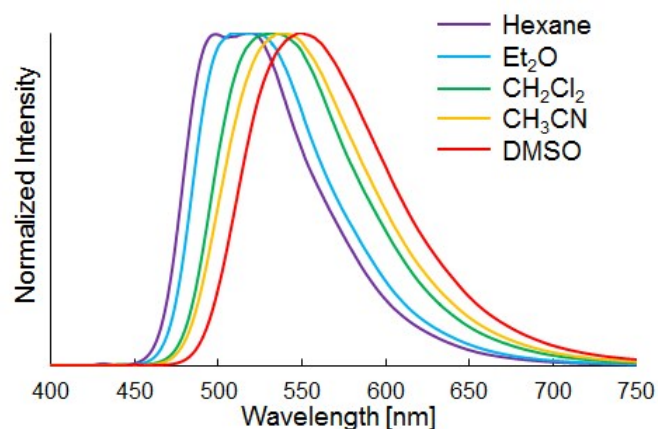
Figure S19. PL spectra of **4e** in various solvents.

Table S7. Optical properties of **4e** in various solvents.

Solvent	$\lambda_{abs}{}^a$ [nm]	$\lambda_{ex}{}^b$ [nm]	$\lambda_{em}{}^c$ [nm]	$\Phi_{PL}{}^d$
Hexane	428	431	510	0.41
Et$_2$O	431	432	515	0.52
CH$_2$Cl$_2$	438	441	535	0.55
CH$_3$CN	436	439	538	0.62
DMSO	446	450	550	0.64

^{a}Longest absorption maximum. ^{b}Excitation maximum (emission at the λ_{em}). ^{c}Emission maximum (excitation at the λ_{ex}).

4. Electronic properties

Table S8. Results of theoretical calculations

	CV[a]			DFT[c]		TD-DFT[c]	
	HOMO [eV]	LUMO [eV]	ΔE [eV]	HOMO [eV]	LUMO [eV]	ΔE [nm]	f
4a	-5.49	-2.21	3.28	-5.30	-2.03	420.48	0.8899
4b	-5.41	-2.28	3.13	-5.44	-2.13	416.75	0.8630
4c	-5.61	-2.54	3.07	-5.77	-2.57	429.57	1.0625
4d	-5.19	-2.32	2.87	-5.03	-1.79	428.56	0.9846
4e	-4.81	-2.13	2.68	-4.63	-1.57	456.80	1.1299
5	-5.74	-2.82	2.92	-5.61	-2.38	432.75	0.7591
6	-[b]	-[b]	-[b]	-6.43	-2.45	350.84	0.1707
7	-[b]	-[b]	-[b]	-5.87	-2.59	426.18	0.7293

[a]CV data were measured in THF solutions (c = 0.1 M) at the scan rate of 10-100 mV/s under N_2. The working electrode was a glassy carbon, the counter electrode was a platinum wire, and the reference electrode was an Ag^0 / Ag^+. E(HOMO) = $-(E_{ox}$ + 4.80) [eV], where E_{ox} is the onset potential of oxidation, observed in the CV analyses. E(LUMO) = $-(E_{red}$ + 4.80) [eV], where E_{red} is the onset potential of reduction, observed in the CV analyses. [c]E_g = E (LUMO) – E(HOMO) [eV]. [b]The data were not obtained because of the decomposition during the measurement.

[c]DFT calculations were carried out to investigate the frontier orbitals of the synthesized compounds. In addition, the HOMO-LUMO transition energies (ΔE) and their oscillator strengths (f) were estimated by TD-DFT calculations. All the calculations employed B3LYP/6-31G+(d,p) (for H, C, N, O, F, S, Cl, As) and LanL2DZ ECP (for As) set combination using the Gaussian 09 program package.
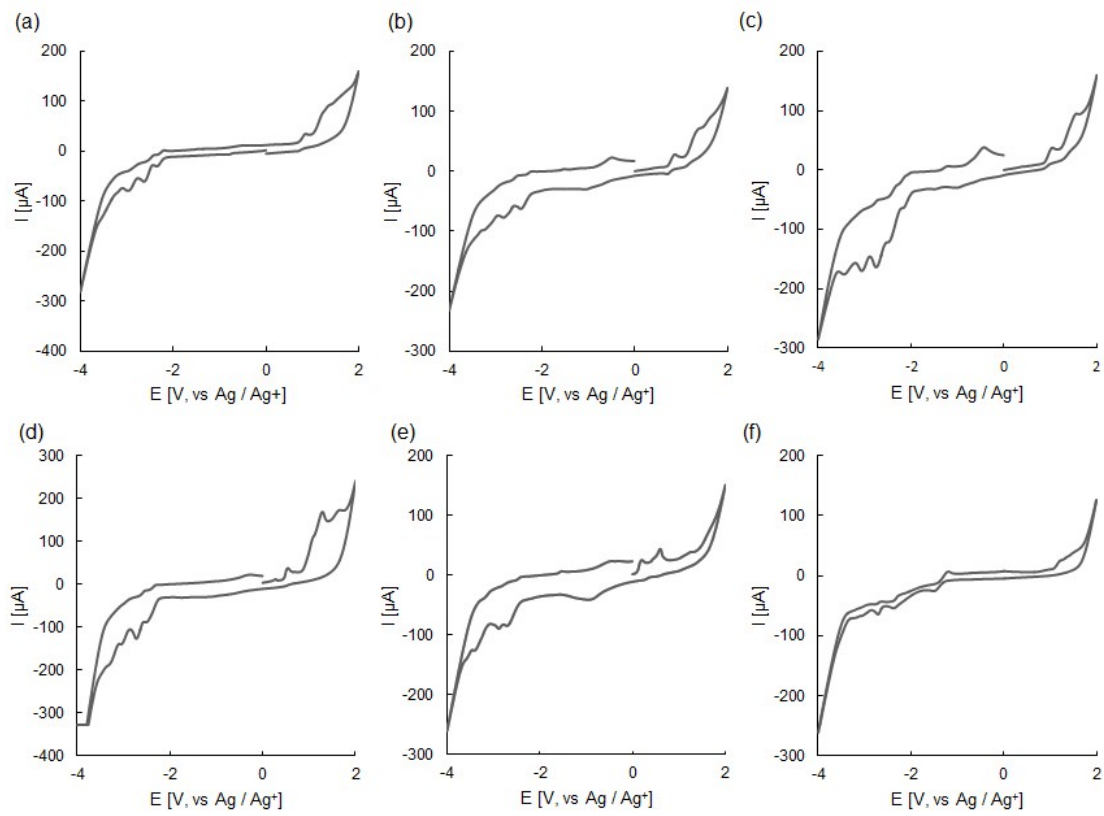
Figure S20. Cyclic voltammograms of (a) **4a** (b) **4b**, (c) **4c**, (d) **4d**, (e) **4e**, and (f) **5** measured in THF solutions ($c = 0.1$ M).